Korea Polymer Journal

Volume 9, Number 1 February 28, 2001

Review

Fully Rod-like Aromatic Polyimides: Structure, Properties, and Chemical Modifications

Moonhor Ree*, Tae Joo Shin, and Seung Woo Lee

Department of Chemistry, Center for Integrated Molecular Systems, BK21 Functional Polymer Thin Film Group, and Polymer Research Institute, Pohang University of Science & Technology, San 31, Hyoja-dong, Pohang 790-784, Korea

Received February 1, 2001

Abstract : Poly(*p*-phenylene pyromellitimide) and poly(4,4'-biphenylene pyromellitimide) are representatives of fully rod-like polyimides. Their structure and properties in thin films are reviewed. The polymers exhibit some excellent properties such as high molecular packing coefficient, high mechanical modulus, and low thermal expansion coefficient, and low interfacial stress, so that they are very attractive to both industry and academia. However, these polymers are very brittle and thus practically useless. Some chemical modifications to improve such drawback with a little sacrifice of the high modulus are described: i) incorporation of short side groups into the polymer backbone and ii) insertion of proper linkages into the polymer backbone.

Introduction

Since a representative polyimide, poly(4,4'-oxydiphenylene pyromellitimide) (PMDA-ODA) was commercialized in early 1960s,[1,2] a number of polyimides have been synthesized and then investigated extensively in the aspect of structure and property relationships.[3-21] In particular, aromatic polyimides have found diverse applications in both microelectronics and aerospace industries as flexible circuitry carriers, stress buffers, interdielectric layers, passivation layers, varnishing resins, fibers, and matrix materials because of their good electrical and mechanical properties, high thermal stability, high chemical resistance, and high dimensional stability.[22-25]

In general, for aromatic polyimides (PIs) without side groups, higher molecular packing coefficient provides higher mechanical modulus as well as low thermal expansion coefficient and low interfacial stress.[8,26-30] Such high property performances are achievable from fully rodlike poly(*p*-

phenylene pyromellitimide) (PMDA-PDA PI) and poly(4,4'-biphenylene pyromellitimide) (PMDA-BZ PI), so that they are so attractive to both industry and academia. However, they are very brittle so that they are practically useless. Thus, there still is a big challenge to improve their brittleness with retaining the high moduli.

Some attempts to improve such drawback with a little sacrifice of the high modulus have been made in two different ways: (i) incorporation of short side groups into the polymer backbone[29-39] and (ii) insertion of proper linkages into the polymer backbone.[6] Such approaches are reviewed, including structure and some other basic properties in addition to mechanical properties.

Incorporation of Short Side Groups

There are two options in incorporating side groups into the polymer rod. One is to incorporate side groups into the diamine moiety while the other is to attach side groups into the dianhydride moiety (see Figure 1). Such side group incorporations are possible through only modification of diamine and dianhydride monomers with side group reactants before synthesizing PI rods, because both PMDA-PDA PI and PMDA-BZ PI are not soluble in most organic solvents and further not moldable and tractable.

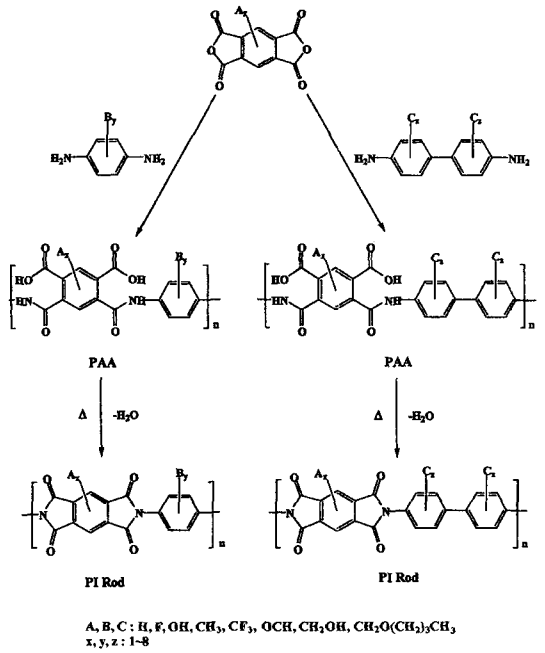

Figure 1. Synthetic scheme of aromatic polyimide rods with and without short side groups.

So far, several *p*-phenylene diamine (PDA) derivatives with short side groups have been developed: 2,5-diaminotoluene (MEPDA), 2,5-diaminoanisole (MEOPDA), 2,5-diaminobenzotrifluoride (CF3PDA), 2,5-diaminofluorobenzene (FPDA), 2,5-diaminote-trafluorobenzene (F4PDA), 1,4-di(hydroxymethyl)-2,5-diaminobenzene (DHOMEPDA), and 1,4-di(*n*-butoxymethyl)-2,5-diaminobenzene (DBMEPDA).[29,34-39] And, some benzidine (BZ) derivatives with short side groups are also available: 2,2'-bis(methyl) benzidine (MEBZ), 2,2'-bis(methoxy)benzidine (MEOBZ), 2,2'-bis(fluoro) benzidine (FBZ), 2,2'-bis(trifluoromethyl)benzidine (CF3BZ), 3,3'-hydroxy-4,4'-diaminobiphenyl (HAB), and *o*-tolidine (TDI).[30,32,35,40]

On the other hand, several research groups[31,33,41-44] have attempted to incorporate short side groups into pyromellitic dianhydride (PMDA). As results of their efforts, some PMDA derivatives are available from only those research groups: 3,6-dimethyloxypyromellitic dianhydride (DMEOPMDA), 1-trifluoromethyl-2,3,5,6-benzenetetracarboxylic dianhydride (CF3DAN), and 1,4-bis(trifluoromethyl) -2,3,5,6-benzenetetracarboxylic dianhydride (DCF3DAN).[31,33,41-44]

From these PMDA, PDA, and BZ derivatives, various PI rods can be synthesized as follows. Fully aromatic PI rods are inherently insoluble in common organic solvents, so that their soluble poly(amic acid) (PAA) precursors are first made by conventional synthetic process. That is, a purified dianhydride monomer is slowly added to a purified diamine monomer of equivalent mole in dry *N*-methyl-2-pyrrolidone (NMP) and followed by stirring for 2 days to make the polymerization mixture homogeneous completely. The obtained PAA precursor solution is filtered and then cast as thin films, finally converted to the corresponding PI films by thermal imidization.

In the same manner, two different series of PI rods were synthesized: i) PMDA-PDA PI analogs PMDA-PDA PI, PMDA-MEPDA PI, PMDA-CF3PDA PI, PMDA-MEOPDA PI, PMDA-F4PDA PI, PMDA-DHOMEPDA PI, PMDA-DBMEPDA

PI, CF3DAN-PDA PI, DCF3DAN-PDA PI, and DMEOPMDA-PDA;[29,31-39,41-44] ii) PMDA-BZ PI analogs PMDA-BZ PI, PMDA-MEOBZ PI, PMDA-MEBZ PI, PMDA-FBZ, PMDA-CF3BZ PI, CF3DAN-BZ PI, CF3DAN-CF3BZ PI, and DCF3DAN-CF3BZ PI.[30-35,40-44] Here, all thermal imidizations were conducted under nitrogen gas flow by a three-step protocol: 150 °C/30 min, 230 °C/30 min, and 380 °C/60 min with a ramping rate of 2.0 K/min per each step.

Insertion of Kink and Bent Linkages

This approach has some freedom in selecting chemical linkage to incorporate into PI rod backbone. Adopting this approach, PMDA, PDA and BZ monomers all can be modified. To retain advantageous properties of PI rod, in practice there is, however, big limitation for such selection. Thus, the modification of either the dianhydride monomer or the diamine monomers would be better than modifying both the dianhydride and the diamines in order to minimize any degradation in the advantageous properties of PI rod. Some dianhydrides can be considered as a modified PMDA monomer, which include biphenyltetracarboxylic dianhydride (BPDA), 4,4'-oxydiphthalic anhydride (ODPA), 3,3',4,4'-benzophenonetetracarboxylic dianhydride (BTDA), and 4,4'-hexafluoroisopropylidenediphthalic anhydride (6F) (see Figure 2). These monomers are available commercially.

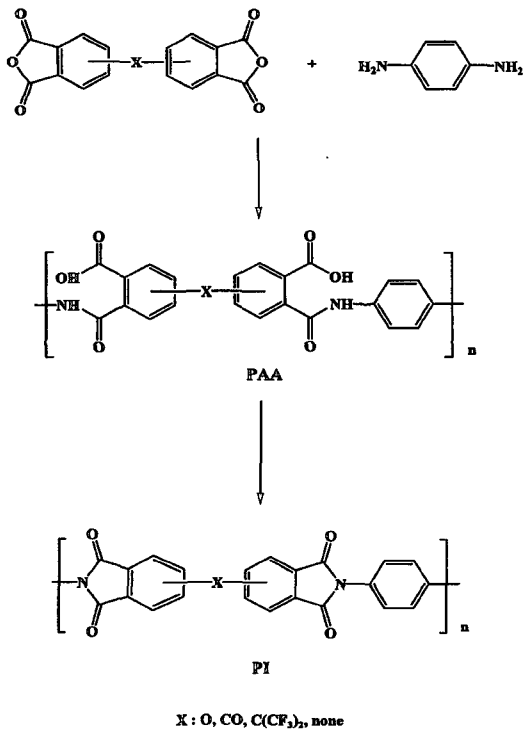

Figure 2. Synthetic scheme of aromatic polyimides containing kink and bent linkages.

From these dianhydrides a series of PAA precursors were synthesized by polycondensations with PDA monomer in the same manner as described in the previous section. Then, PAA solutions were cast and dried, finally imidized under nitrogen flow by a three-step protocol (i.e., 150 °C/30 min, 230 °C/30 min, 300 °C/30 min and 400 °C/1.5 h with a ramping rate of 2.0 K/min):6 PMDA-PDA PI, BPDA-PDA PI, ODPA-PDA PI, BTDA-PDA PI, and 6F-PDA PI (see Figure 2).

Structure

PMDA-PDA. PI Derivatives. Figure 3 illustrates X-ray diffraction patterns from PMDA-PDA PI analogs in films.[29,35] PMDA-PDA PI reveals a reflection pattern showed only two peaks, one big, broad peak at 20.7° (2θ) and another weak, broad peak at about 25.6°, consequently showing no regularly ordered structure. The peak at 20.7° is the amorphous halo, giving a *d*-spacing of 4.3 Å which corresponds to the average intermolecular distance in the direction of film thickness. The transmission pattern exhibits an amorphous halo peak as well as multiple (00*l*) peaks. The amorphous halo peak at 18.8°, gives a *d*-spacing of 4.7 Å which corresponds to the average intermolecular distance in the film plane. This mean intermolecular distance is larger than that in the direction of film thickness, indicating that the rod-like polymer chains in the thin film are packed more loosely in the film plane than the direction of film thickness. The multiple (00*l*) peaks are (001) peak at 7.26° (12.2 Å), (002) peak at 14.6° (6.1 Å), (003) peak at 21.6° (4.1 Å), (004) peak at 29.1° (3.1 Å), (005) peak at 36.6° (2.5 Å), and (006) peak at 44.4° (2.0 Å). From the (00*l*) peaks, there are possible at least three structural informa-

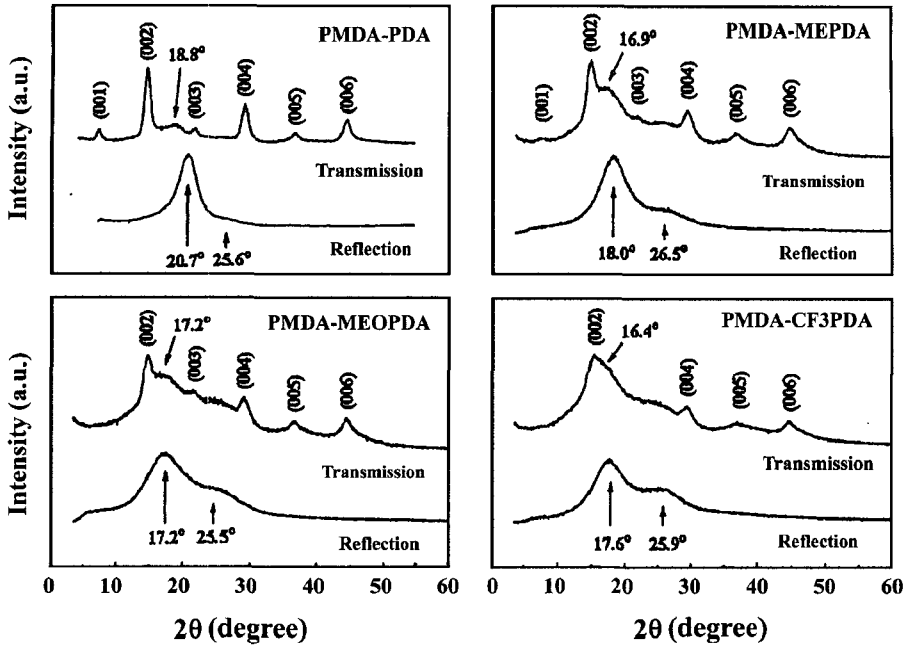

Figure 3. Reflection and transmission X-ray diffraction patterns of PMDA-PDA PIs with side groups in thin films. The Cu K_α radiation source was used.

tion as follows. First, the length of repeating unit projected along the chain axis is estimated to be 12.2 Å. Second, the appearance of (00*l*) peaks might result from the polymer chains ordered in bundles without any lateral ordering. Coherence length (L_C) is estimated from the Scherrer equation[45] to be 130 Å for the (002) peak and 33.6 Å for the amorphous halo peak. Therefore, the polymer chains ordered in bundles are speculated to be in a dimension of 130 Å length and 33.6 Å diameter. Third, the (00*l*) peaks appear only in the transmission pattern, indicating that the polymer chains are oriented preferentially in the film plane.

Similar WAXD patterns are observed for PMDA-MEPDA PI, PMDA-CF3PDA PI, and PMDA-MEOPDA PI. All the polymer chains are favorably aligned in the film plane, regardless of incorporating side groups. However, all diffraction peaks become broad and weak, and the mean intermolecular distances increase, depending on the side groups. For PMDA-MEPDA PI, L_C is 77 Å for the (002) peak and 15.1 Å for the amorphous halo peak, whereas the mean intermolecular distance is 4.9 Å in the direction of film thickness and 5.2 Å in the film plane. For PMDA-MEOPDA PI, L_C is 74 Å for the (002) peak and 11.7 Å for the amorphous halo peak, whereas the mean intermolecular distance is 5.2 Å in the direction of film thickness and 5.2 Å in the film plane. For PMDA-CF3PDA PI, L_C is 63 Å for the (002) peak and 13.8 Å for the amorphous halo peak, whereas the mean intermolecular distance is 5.0 Å in the direction of film thickness and 5.0 Å in the film plane. Unlike the other PIs, PMDA-MEOPDA PI reveals the same mean intermolecular distance in the film plane and in the direction of film thickness. This might be attributed to the relatively bulky methoxy side group on the backbone.

As discussed above, all the PI rods are ordered like bundles, but not laterally packed in a regular way. Such bundle-like interchain ordering is decreased in size by the incorporation of side groups. The effect of side group on the interchain ordering is in the increasing order PMDA-PDA PI < PMDA-MEPDA PI < PMDA-MEOPDA PI < PMDA -CF3PDA PI. In addition, the mean intermolecular distance increases as the bulkiness of side group increases, resulting in a reduction in the chain packing density.

Besides the diffraction peaks described above, it is worthy to pay attention on the shoulder diffraction peak around 25.5-26.5° in the reflection pattern. This peak is considered to relate to the intermolecular packing order, along with the diffraction peak around 17.2-20.7°. The peak is very weak, broad for the PMDA-PDA PI. However, the peak is enhanced in intensity by incorporating side groups. The intensity enhancement is in the increasing order PMDA-PDA PI < PMDA-MEPDA PI < PMDA-MEOPDA PI < PMDA-CF3PDA PI. This suggests that the degree of interchain ordering is increased by incorporating side groups. This might originate from the chain mobility improved by rotational freedom due to the side groups as well as the intermolecular interaction via the side groups.

With these X-ray diffraction results, densities are measured and listed together in Table I.[29,35] Density is in the increasing order PMDA-MEPDA PI < PMDA-MEOPDA PI < PMDA-PDA PI < PMDA-CF3PDA PI. In particular, PMDA-CF3PDA PI exhibits the highest density, which results from heavy fluorine atoms of the side group despite its bulkiness. In contrast, PMDA-MEPDA PI shows the lowest density, which is contributed by the light hydrogen atoms of the side group in spite of its relatively low bulkiness.

From the densities, molecular packing coefficients can be estimated using the following relationship proposed by Slonimskii *et al.*:[46]

$$K = \frac{V_{int}}{V_{true}} \quad (1)$$

$$= \frac{N_A \sum \Delta V_i}{M/d} \quad (2)$$

Here, V_{int} is the total intrinsic volume of the atoms consisting of the repeating unit, V_{true} the molar volume calculated from the density d, ΔV_i the volumetric increment of atoms, M the molecular weight of repeating unit, and N_A Avogadro's number.

The results are listed in Table I.[29,35] Molecular packing coefficient (K) is in the increasing order PMDA-CF3PDA PI < PMDA-MEOPDA PI < PMDA-MEPDA PI < PMDA-PDA PI. That is, the incorporation of side group disturbs the packing coefficient of polymer chains. The disturbance of molecular packing increases significantly as the bulkiness of side group increases.

PMDA-BZ PI Derivatives. X-ray diffraction patterns of PMDA-BZ PI analogs in films are illustrated in Figure 4.[30,32] PMDA-BZ PI exhibits the first diffraction peak at 5.30° (2θ) (16.66 Å d-spacing) in the transmission pattern, which corresponds to the length of the chemical repeat unit on the fully extended polymer chain. Its highly ordered (00l) peaks appear, too as detected from PMDA-PDA PI. In addition, an additional peak with broadness appears at 18.7°, which is the amorphous halo. In contrast, the reflection pattern shows only an amorphous halo peak at 21° (2θ). The (00l) peaks appeared only in the transmission pattern suggest that the rodlike polymer chains are assembled together as bundles and such bundles are preferentially aligned in the film plane. In addition, the absence of any other lateral order peak except for the amorphous halo indicates that the bundles composed of the rodlike polymer chains do not have any regular order in the lateral direction. Such absence of lateral packing order is also detected in the reflection pattern.

The (001), (002) and (003) peak have L_C's of

Table I. Densities, Packing Coefficients and Thermal Properties of PMDA-PDA PIs Containing Short Side Groups

PI Film[a]	Density (g/cm^3)	Packing coefficient K	In-plane TEC (ppm/°C)	T_g[b] (°C)	T_d[c] (°C)
PMDA-PDA	1.500	0.715	-	-	570
PMDA-MEPDA	1.427	0.697	1.6	368	450
PMDA-MEOPDA	1.438	0.692	0.4	365	430

[a]Film thickness : 10-11.5 μm.

[b]Glass transition temperature.

[c]Degradation temperature.

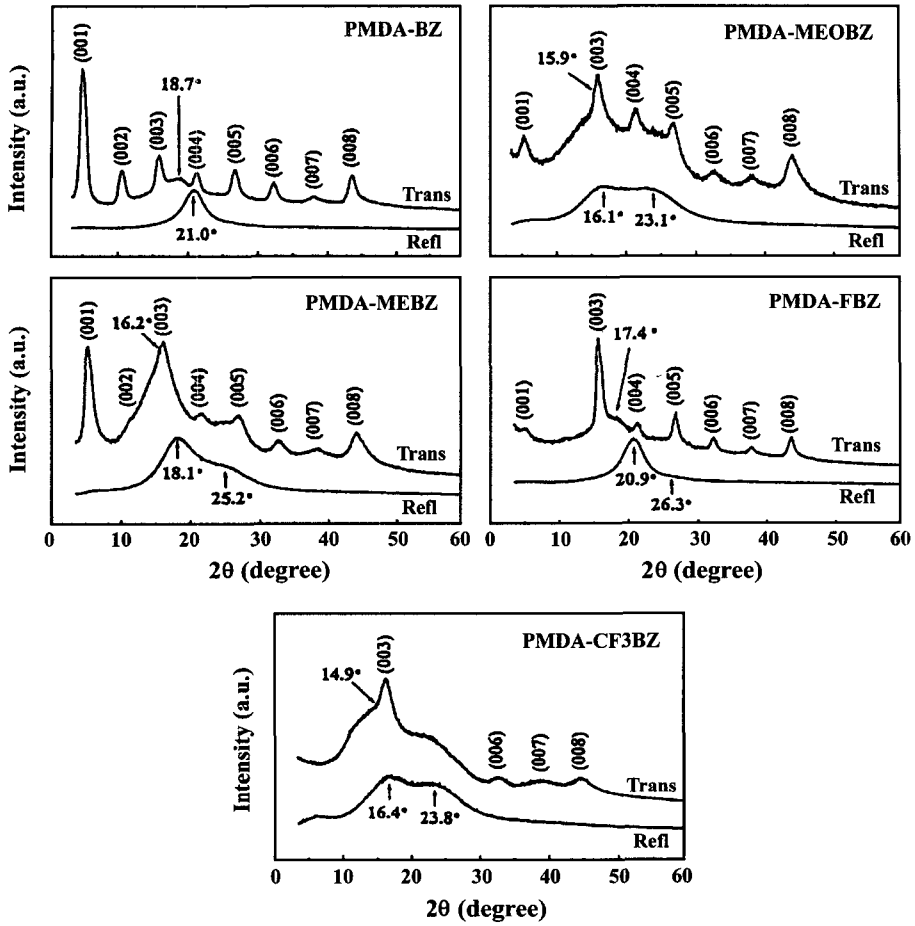

Figure 4. Reflection and transmission X-ray diffraction patterns of PMDA-BZ PIs with side groups in thin films. The Cu K_α radiation source was used.

81.5, 79.5 and 87.2 Å, respectively, giving an averaged L_C of 82.7 Å. The amorphous halo in the transmission pattern has a *d*-spacing of 4.75 Å (that is, the mean interchain distance in the film plane) and a L_C of 16.3 Å, whereas the amorphous halo exhibits a *d*-spacing of 4.23 Å (i.e., the mean interchain distance in the direction of film thickness) and a L_C of 27.2 Å. These results suggest that the polymer chains assemble together as bundle-like ordered phases in a dimension of $82.7 \times 16.3 \times 27.2$ Å, which contains 5 chemical repeat units along the chain axis, 3-4 polymer chains in the lateral direction in the film plane, and 6-7 polymer chains in the lateral direction in the direction normal to the film plane. It is also noted that the in-plane oriented polymer chains are packed more densely in the direction of film thickness than in the film plane.

Similar X-ray diffraction patterns are detected for PMDA-FBZ PI. As observed for the PMDA-BZ PI, the (00*l*) peaks are detected only in the transmission pattern, indicative of the preferential in-plane orientation of the polymer chains. In particular, the (002) peak was weakened very much in the intensity. The mean interchain distance is estimated to be 5.08 Å in the film plane and 4.24 Å in the direction of film thickness. The dimension of the bundle-like ordered phases is estimated to be $83.7 \times 14.1 \times 24.9$ Å which corresponds to 5 chemical units along the chain axis, 2-3 polymer chains in the film plane and 5-6 polymer chains in the direction of film thickness.

PMDA-MEOBZ PI also revealed (00*l*) peaks nicely in the transmission pattern, but did not show any (*hkl*) diffraction related to a regular packing order in the lateral direction except for the amorphous halo at 15.9°. This pattern is apparently similar to that of the PMDA-BZ PI. However, the (00*l*) peaks of PMDA-MEOBZ PI are relatively board and weak. In particular, the (002) peak is weakened very much so that it apparently is not distinguishable. A *d*-spacing is calculated to be 16.11 Å for the (001) peak, which is very close to that of PMDA-BZ PI. The averaged L_C estimated from the (001), (002) and (003) peak is 66.9 Å. For the amorphous peak, a *d*-spacing of 5.58 Å and a L_C of 11.8 Å are estimated. The reflection pattern shows no (00*l*) peaks as observed for the PMDA-BZ PI, indicative of the preferential in-plane orientation of the polymer chains. However, the reflection pattern showed two distinctive peaks: one peak is at 16.1° and another at 23.1°. For the first peak at 16.1° which is considered as the first order amorphous halo, a *d*-spacing of 5.49 Å and a L_C of 14.2 Å are estimated. These results suggest that the bundle-like ordered phases have a size of 66.9× 11.8× 14.2 Å which corresponds to 4 chemical units along the chain axis, 2 polymer chains in the film plane and 2-3 polymer chains in the direction of film thickness. This size of the ordered phases is relatively smaller than that of the PMDA-BZ PI. However, PMDA-MEOBZ PI reveals two diffraction peaks in the reflection pattern, differently from the PMDA-BZ PI. These two peaks are directly correlated to the molecular packing order in the lateral direction. Thus, the appearance of the second peak in a distinctive intensity may be indication that the overall molecular packing order in the lateral direction is enhanced in an appreciable level even though the dimension of the ordered phases are slightly smaller than those in the PMDA-BZ PI.

PMDA-MEBZ PI shows X-ray diffraction patterns similar to those of the PMDA-MEOBZ PI. The size of the bundle-like ordered phases is estimated to be 71.9× 15.1× 15.4 Å which corresponds to 4-5 chemical units along the chain axis, 2-3 polymer chains in the film plane and 3 polymer chains in the direction of film thickness. The mean interchain distance is estimated to be 5.45 Å in the film plane and 4.89 Å in the direction of film thickness. In particular, it is noted that two peaks rather than one peak appear in the reflection pattern and, however, the intensity of the second peak in the high angle region is relatively weaker than that of the PMDA-MEOBZ PI.

Similar WAXD patterns are also observed for PMDA-CF3BZ PI. The reflection pattern is very close that of the PMDA-MEOBZ PI in the shape. However, the (00*l*) peaks in the transmission pattern are relatively weakened and, furthermore, the (001), (002), (004) and (005) peaks apparently are not distinguishable. The dimension of the bundle-like ordered phases is estimated to be 53.2 × 11.5 × 13.3 Å which corresponds to 3-4 chemical units along the chain axis, 2 polymer chains in the film plane and 2-3 polymer chains in the direction of film thickness. The mean interchain distance is estimated to be 5.96 Å in the film plane and 5.39 Å in the direction of film thickness.

In comparison, both size and population of the bundle-like ordered phases increase in the order PMDA-CF3BZ PI < PMDA-MEOBZ PI < PMDA-MEBZ PI < PMDA-FBZ PI < PMDA-BZ PI, respectively. The mean interchain distance in the film plane is in the increasing order PMDA-BZ PI < PMDA-FBZ PI < PMDA-MEBZ PI < PMDA-MEOBZ PI < PMDA-CF3BZ PI, whereas that in the direction of film thickness is in the increasing order PMDA-BZ PI ≈ PMDA-FBZ PI < PMDA-MEBZ PI < PMDA-CF3BZ PI < PMDA-MEOBZ PI. The intensity of the second peak in the reflection pattern increases in the order PMDA-BZ PI ≈ PMDA-FBZ PI < < PMDA-MEBZ PI < PMDA-MEOBZ PI ≈ PMDA-CF3BZ PI.

In addition, densities were measured. The results are listed in Table II. Densities are in the range of 1.34-1.51 g/cm^3, depending upon the side groups. In comparison, density is in the decreasing order PMDA-FBZ PI > PMDA-CF3BZ PI > PMDA-BZ PI > PMDA-MEOBZ PI > PMDA-MEBZ PI.[30,32] In fact, the volume and weight of a substituent contribute competitively to the density. Thus, the relatively high densities of PMDA-FBZ PI and PMDA-CF3BZ PI result from the heavy fluorine atoms of the side groups despite their bulkinesses. In contrast, the low densities of PMDA-MEBZ PI and PMDA-MEOBZ PI are due to the light hydrogen

Table II. Densities, Packing Coefficients and Thermal Properties of PMDA-BZ PIs Containing Short Side Groups

PI Film[a]	Density (g/cm^3)	Packing Coefficient K	In-plane TEC (ppm/°C)	T_g[b] (°C)	T_d[c] (°C)
PMDA-BZ	1.46	0.720	-1.5	-	580
PMDA-MEOBZ	1.39	0.689	-2.2	328	430
PMDA-MEBZ	1.34	0.685	-6.9	355	490
PMDA-FBZ	1.51	0.698	-1.7	398	600
PMDA-CF3BZ	1.49	0.640	-2.5	358	520

[a]Film thickness: 9.3-14.3 μm.

[b]Glass transition temperature.

[c]Degradation temperature.

atoms of the side groups in addition to their bulkinesses. Molecular packing coefficients are estimated from the densities using Eq. (2). The results are listed in Table II. Molecular packing coefficient K decreases in the order PMDA-BZ PI > PMDA-FBZ PI > PMDA-MEOBZ PI > PMDA-MEBZ PI > PMDA-CF3BZ PI.[30,32] That is, the incorporation of side groups decreased the packing coefficient of polymer chains. In general, one can easily expect that the effect of side group on the disturbance of molecular packing increases significantly as the bulkiness of side group increases. However, PMDA-MEOBZ PI has a slightly higher packing coefficient than that of PMDA-MEBZ PI in spite of its methoxy side group relatively larger than methyl side group. This may result from the difference between the thermal imidization temperatures of the two PIs: the PMDA-MEOBZ PI was imidized at 380 °C and, however, the PMDA-MEBZ PI was imidized at 350 °C. Overall, for a given PI system, higher imidization temperature produces higher density in the resultant PI.

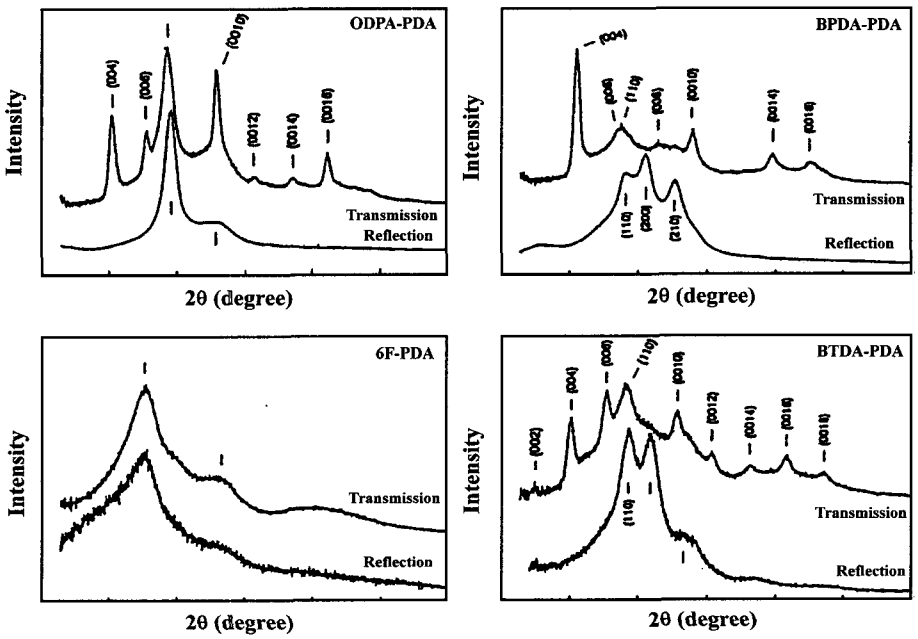

Figure 5. Reflection and transmission X-ray diffraction patterns of PDA-based PIs containing various linkages in thin films. The Cu K_α radiation source was used.

PDA-Based PI Derivatives. X-ray diffraction patterns of this series of PIs in films[6] are presented in Figure 5. X-ray diffractions of PMDA-PDA PI were already described above. Similar diffraction patterns are obtained for ODPA-PDA PI. Its transmission pattern reveals mostly (00*l*) peaks: (004) at 10.62° (8.3 Å), (006) at 15.65° (5.7 Å), (0010) at 26.1° (3.4 Å), (0012) at 31.5° (2.8 Å), (0014) at 37.2° (2.4 Å), and (0016) at 42.3° (2.1 Å). This indicates that ODPA-PDA PI chains are highly ordered along the polymer chain axis and, furthermore, the extended polymer chains are stacked together in a certain scale. The monomer repeat length projected along the chain axis is estimated from these (00*l*) peaks to be 16.9 Å. The coherence length of the (004) peak is 95 Å. The mean intermolecular distance is estimated from the peak at 18.80° to be 4.7 Å. In addition, in the reflection pattern the mean intermolecular distance is estimated to be 4.6 Å (19.23°), which is very close to that in the transmission pattern. The PI molecules are also oriented in the film plane with no regular chain ordering as observed for PMDA-PDA PI.

However, BPDA-PDA PI and BTDA-PDA PI show X-ray diffraction patterns different from those of PMDA-PDA PI and ODPA-PDA PI described above. BPDA-PDA PI reveals (*hkl*) peaks, which are not observed for PMDA-PDA PI and ODPA-PDA PI, in addition to the (00*l*) peaks. According to previous X-ray diffraction measurements and structural refinement analysis,[47,48] BPDA-PDA PI chains form crystals that are based on the orthorhombic crystal unit cell with a space group of *Pba2*. The diffraction peaks are indexed in accordance to the previous results.[47,48] Five distinct (00*l*) peaks, which are not detected on the reflection pattern, appeared on the transmission pattern: (004) at 11.13° (7.9 Å), (008) at 22.36° (4.0 Å), (0010) at 27.92° (3.2 Å), (0014) at 39.62° (2.3 Å), and (0016) at 45.22° (2.0 Å). This indicates that highly ordered BPDA-PDA PI chains are also aligned preferentially in the film plane. From the d-spacings of these (00*l*) peaks, the monomer repeat length projected along the chain axis is estimated to be 16.0 Å. The coherence length of the (004) peak is calculated to be 104 Å. The reflection reveals only three (*hkl*) peaks, such as (110) at 18.37° (4.8 Å), (200) at 21.25° (4.2 Å), and (210) at 25.4° (3.5 Å), indicating that the in-plane oriented polymer chains are regularly well ordered. The mean intermolecular distance, which is estimated from the (110) peak, is 4.9 Å (18.09°) in the transmission pattern and 4.8 Å (18.37°) in the reflection pattern.

Like BPDA-PDA PI, BTDA-PDA PI reveals a relatively high chain order. Relatively sharp eight (00*l*) peaks appear together with the (110) peak on the transmission pattern: (002) at 4.95° (17.8 Å), (004) at 10.27° (8.6 Å), (006) at 15.34° (5.8 Å), (0010) at 25.73° (3.5 Å), (0012) at 30.80° (2.9 Å), (0014) at 36.37° (2.5 Å), (0016) at 41.57° (2.2 Å), (0018) at 47.14° (1.9 Å) and (110) at 18.31° (4.8 Å). The reflection pattern shows two distinct peaks (18.68° and 21.77°) and several weak peaks at 25-40° corresponding to (*hkl*) diffractions, but does not reveal the (00*l*) peaks as observed in the transmission pattern. That is, BTDA-PDA PI molecules are oriented in the film plane and regularly well ordered. The mean intermolecular distance is 4.8 Å (18.31°) in transmission and 4.7 Å (18.68°) in reflection. The monomer repeat length projected along the chain axis is estimated to be 17.4 Å. The coherence length of the (004) peak is estimated to be 98 Å.

Unlike PIs described above, 6F-PDA PI reveals structureless WAXD patterns. 6F-PDA PI shows three broad peaks in the reflection as well as the transmission geometry: the first one at 15.34°, the second at ca. 26.6°, and the third at ca. 41° (2θ). The first diffraction peak at 15.34° can be assigned as the first order amorphous halo, consequently giving the mean intermolecular distance of 5.8 Å. Except for the di(trifluoromethyl) group instead of the carbonyl oxygen on the methylene unit of the backbone, its chemical structure is similar to that of BTDA-PDA. For this reason, its monomer repeat distance projected along the extended chain axis is assumed to be same as that (17.4 Å) of BTDA-PDA. Its chain order seems to be similar with that of BTDA-PDA. However, such chain order does not appear in X-ray diffraction patterns. In addition, such high in-plane orientation of polymer chains, as observed for the polyimides descibed above, is not detected for 6F-PDA. These might result from very poor chain ordering

caused by the bulky di(trifluoromethyl) groups.

In comparison, the coherence length along the chain axis follows in increasing order 6F-PDA (could not be measured) < ODPA-PDA PI (95 Å) < BTDA-PDA PI (98 Å) < BPDA-PDA PI (104 Å) < PMDA-PDA PI (130 Å). The coherence length, which is estimated from the broadening of (00*l*) peaks, is a function of the size of crystals along the chain axis as well as the degree of disorder in the crystals. The crystal size is a function of Kuhn length,[49] which is a measure of chain rigidity: Higher Kuhn length indicates higher chain rigidity. Therefore, one expects that higher chain rigidity can give higher crystal size along the chain axis, leading to higher coherence length. However, lower coherence length would be expected for crystals with poor chain ordering, that is high degree of disordering, even though a polymer exhibits very high chain rigidity. PMDA-PDA PI is a fully rodlike polymer so that its Kuhn length can be simply calculated to be 1452 Å from the projected repeat unit distance (11.9 Å) and the degree of polymerization (122 = 40,000/326 where molecular weights of the precursor polymer and its repeat unit are 40,000 and 326, respectively). In addition, according to theoretical calculations of Birshtein and Goryunov,[50] Kuhn length is 118 Å for BPDA-PDA PI, 44 Å for ODPA-PDA PI, and 34 Å for BTDA-PDA PI. The Kuhn length of 6F-PDA PI is presumed to be ca. 34 Å because of its backbone structure similar to BTDA-PDA PI except that it has a hexafluoroisoporpylidene carbon linkage instead of the carbonyl carbon linkage. From these data, Kuhn length is in the increasing order 6F-PDA PI ≈ BTDA-PDA PI < ODPA-PDA PI < BPDA-PDA PI < PMDA-PDA PI.

BTDA-PDA PI, which has relatively smaller Kuhn length than ODPA-PDA PI, exhibits much better chain ordering, resulting in slightly larger coherence length. The coherence length of 6F-PDA PI, which exhibits a Kuhn length comparable to that of BTDA-PDA PI but exhibits very poor chain ordering due to the bulky di(trifluoromethyl) group, could not be detectable in diffraction patterns. In addition, PMDA-PDA PI, which is expected to have an extremely large Kuhn length of 1452 Å, revealed only a very limited coherence length of 130 Å, which might result from a limited chain ordering caused by highly restricted mobility of the rodlike polymer chain having higher glass transition than the decomposition temperature. These indicate that the coherence length along the chain axis strongly depends not only on the chain rigidity but also on the ordering of chain. Therefore, it is suggested that higher chain rigidity and ordering lead higher coherence length in the solid state of aromatic PIs.

The mean intermolecular distance, which is a parameter of molecular packing, is in the increasing order PMDA-PDA PI (4.2-4.7 Å) < ODPA-PDA PI (4.6-4.7 Å) < BTDA-PDA PI (4.7-4.8 Å) < BPDA-PDA PI (4.8-4.9 Å) < 6F-PDA PI (5.8 Å). For all PIs except for 6F-PDA PI, the mean intermolecular distance is shorter in the out-of-plane than in the film plane. That is, for the thin film composed of highly in-plane oriented polymer chains, polymer chains are more densely packed together in the out-of-plane than in the film plane. However, for 6F-PDA PI its mean intermolecular distance in the film plane is almost same with that in the out-of-plane.

Optical and Dielectric Properties

PMDA-PDA PI Derivatives. In-plane and out-of-plane refractive indices (n_{xy} and n_z), which were measured at 632.8 nm (474.08 THz in optical frequency), are listed in Table III.[29,35,51,52] In comparison, n_{xy} is in the increasing order PMDA-CF3PDA PI < PMDA-MEOPDA PI < PMDA-MEPDA PI < PMDA-PDA PI, whereas n_z is also in the increasing order PMDA-CF3PDA PI < PMDA-PDA PI < PMDA-MEOPDA PI < PMDA-MEPDA PI. All PI films show n_{xy} larger than n_z, regardless of the side groups. This indicates two things as follows. First, these PIs are positively birefringent polymers. That is, the polarizability along the chain axis is higher than that normal to the chain axis. Birefringence ($\Delta = n_{xy} - n_z$) in the thin film is in the increasing order PMDA-CF3PDA PI < PMDA-MEOPDA PI < PMDA-MEPDA PI < PMDA-PDA PI. Second, all the PI chains are preferentially aligned in the film plane. These are consistent with the results observed in the X-ray diffraction study as described above.

The average refractive index [$n_{av} = (2n_{xy} + n_z)/3$]

is in the increasing order PMDA-CF3PDA PI < PMDA-MEOPDA PI < PMDA-MEPDA PI < PMDA -PDA PI.

These refractive indices are attributed to the polarizabilities of atoms consisting of polymer backbones and their chemical bonds. In general, higher polarizability causes higher dipole moment under electromagnetic field, providing higher refractive index. The fluorine atom exhibits a relatively low polarizability because of its high electronegativity and small volume, whereas the carbon atom presents large polarizability.[44,53] Both oxygen and hydrogen have intermediate polarizabilities.[44,53] When these atoms involve in the formation of chemical bonds, the polarizabilities of the chemical bonds also contribute to the refractive index. Therefore, the incorporation of low polarizable atoms, as well as low polarizable chemical bonds into the polymer chain can reduce the refractive index. PMDA-CF3PDA PI shows the lowest refractive index, which is contributed from the trifluoromethyl side group. In fact, for this polymer, the fluorine atoms contribute positively to the reduction of refractive index and, however, their chemical bonds to the carbon atom contribute negatively because of the relatively high polarizabilities caused by the large difference between the electronegativities of fluorine and carbon atom. However, from the result it is evident that in the reduction of refractive index the former contribution is higher than the latter one.

Therefore, the relatively low refractive indices of the PMDA-PDA PIs containing side groups are overall attributed to the incorporations of side groups containing fluorine, oxygen and hydrogen atoms that have relatively lower polarizabilities than that of carbon atom. In comparison, the contribution in the reduction of refractive index is high for the trifluoromethyl group, intermediate for the methoxy group and low for the methyl group. In addition, the reduction of refractive index due to the incorporation of side group is also contributed in part from an increase in the free volume of the polymer caused by the steric bulkiness of side group. That is, the side group with a steric bulkiness leads to a less efficient packing of the polymer chains, resulting in an increase of free volume in the polymer film.

Dielectric constants of the PIs can be estimated from the measured refractive indices using Maxwell equation ($\varepsilon = n^2$).[54] The results are illustrated in Table III. Here, it is noteworthy that the dielectric constants, which were obtained at the optical frequency, are attributed mainly to electronic polarization and in part to atomic polarization: The dipole orientation polarization would not contribute to the dielectric constants because of its limited slow process.[55] PMDA-PDA PI exhibits the highest in-plane and average dielectric constant (ε_{xy} and ε_{av}), whereas PMDA-MEPDA PI shows the highest out-of-plane dielectric constant (ε_z). In contrast, PMDA-CF3PDA PI exhibits the lowest ε_{xy}, ε_z, and ε_{av}. In addition, this PI shows the lowest anisotropy in the dielectric constant. Large anisotropy in the dielectric constant often causes near-coupled-noise due to crosstalks in the performance of microelectronic devices.[22,24] Therefore, PMDA-CF3PDA PI may be suitable for the applications in microelectronic devices because of the low dielectric constant and anisotropy.

PMDA-BZ PI Derivatives. Table IV presents n_{xy}'s and n_z's of PMDA-BZ PI analogs in thin

Table III. Optical and Dielectric Properties of PMDA-PDA PIs Containing Short Side Groups

PI Film[a]	Optical Properties[b]				Dielectric Properties[c]			
	n_{xy}	n_z	n_{av}	Δ	ε_{xy}	ε_z	ε_{av}	$\Delta\varepsilon$
PMDA-PDA	1.823	1.582	1.743	0.241	3.323	2.503	3.038	0.820
PMDA-MEPDA	1.751	1.595	1.699	0.156	3.066	2.544	2.877	0.522
PMDA-MEOPDA	1.743	1.589	1.692	0.154	3.038	2.525	2.863	0.513
PMDA-CF3PDA	1.678	1.556	1.637	0.122	2.816	2.421	2.680	0.395

[a]Film thickness: 10.0-11.5 μm.

[b]Measured at 632.8 nm (474.08 THz).

[c]Estimated from refractive indices using Maxwell equation ($\varepsilon = n^2$).

films.[30,32] These PIs also exhibit n_{xy} larger than n_z as observed in PMDA-PDA PI analogs. This indicates that all the PIs are the positively birefringent polymers in which the polarization along the chain axis is higher than that normal to the chain axis. In comparison, n_{xy} is in the decreasing order PMDA-BZ PI > PMDA-FBZ PI > PMDA-MEBZ PI > PMDA-MEOBZ PI > PMDA-CF3BZ PI, whereas n_z is in the decreasing order PMDA-MEOBZ PI > PMDA-BZ PI > PMDA-MEBZ PI > PMDA-FBZ PI > PMDA-CF3BZ PI. n_{av} decreases in the order PMDA-BZ PI > PMDA-FBZ PI > PMDA-MEBZ PI > PMDA-MEOBZ PI > PMDA-CF3BZ PI. Δ is in the decreasing order PMDA-BZ PI > PMDA-FBZ PI > PMDA-MEBZ PI > PMDA-MEOBZ PI > PMDA-CF3BZ PI.

Overall, the incorporation of side groups on the polymer backbone lowers n_{xy} and n_z of the PMDA -BZ PI film, resulting in the decreases in both the bulk refractive index n_{av} and the optical anisotropy Δ. The effect of side group to the optical properties is rated in the increasing order H (hydrogen) < F < CH_3 < OCH_3 < CF_3. This result can be understood with considering chemical and structural characteristics of the side groups as discussed in the previous section. In conclusion, the refractive index of PMDA-BZ PI is reduced by the incorporation of side groups having relatively low polarizabilities and large bulkiness.

From the measured refractive indices, dielectric constants and anisotropies are also estimated and summarized in Table IV. With considering dielectic constants and their anisotropy, PMDA-CF3BZ PI is a good candidate material to fabricate microelectronic devices. From the results, again it is suggested that the incorporation of short side groups having very low polarizability, such as CF_3 and other perfluorinated short alkyls, into a rodlike polymer backbone is one of the most useful routes to make high preformance polyimides which can exhibit isotropically low refractive index and dielectric constant.

PDA-Based PI Derivatives. As listed in Table V, all the PI films also show n_{xy} larger than n_z, resulting in an optical anisotropy.[6] Δ is 0.2333 for BPDA-PDA PI, 0.1430 for ODPA-PDA PI, 0.1309 for BTDA-PDA PI, and 0.0112 for 6F-PDA PI. PMDA-PDA PI with the highest chain rigidity exhibits the largest optical anisotropy, whereas 6F-PDA PI, which is structureless with the lowest

Table IV. Optical and Dielectric Properties of PMDA-BZ PIs Containing Short Side Groups

PI Film	Optical Properties[b]				Dielectric Properties[c]			
	n_{xy}	n_z	n_{av}	Δ	ε_{xy}	ε_z	ε_{av}	$\Delta\varepsilon$
PMDA-BZ	1.851	1.591	1.764	0.260	3.426	2.531	3.113	0.895
PMDA-MEOBZ	1.745	1.598	1.693	0.156	3.045	2.555	2.867	0.490
PMDA-MEBZ	1.753	1.579	1.695	0.174	3.071	2.492	2.872	0.579
PMDA-FBZ	1.805	1.575	1.729	0.230	3.258	2.482	2.989	0.776
PMDA-CF3BZ	1.636	1.512	1.595	0.124	2.677	2.286	2.543	0.390

[a]Film thickness: 9.3-14.3 μm.

[b]Measured at 632.8 nm (474.08 THz).

[c]Estimated from refractive indices using Maxwell equation ($\varepsilon = n^2$).

Table V. Optical and Dielectric Properties of Films of PDA-based PIs with Various Chain Rigidities

PI Film[a]	Optical Properties[b]				Dielectric Properties[c]			
	n_{xy}	n_z	n_{av}	Δ	ε_{xy}	ε_z	ε_{av}	$\Delta\varepsilon$
BPDA-PDA	1.8474	1.6141	1.7696	0.2333	3.413	2.605	3.132	0.808
ODPA-PDA	1.7801	1.6371	1.7324	0.1430	3.169	2.680	3.001	0.489
BTDA-PDA	1.7692	1.6383	1.7256	0.1309	3.130	2.684	2.978	0.446
6F-PDA	1.5847	1.5762	1.5819	0.0112	2.511	2.484	2.502	0.027

[a]Film thickness: 10.0-11.5 μm.

[b]Measured at 632.8 nm (i.e., 474.08 THz).

[c]Estimated from refractive indices using Maxwell equation ($\varepsilon = n^2$).

rigidity, reveals the lowest optical anisotropy. The others exhibit intermediate optical anisotropies. These anisotropies result from the in-plane orientation of polymer chains in which the principal polarization is along the chain axis. This is directly correlated to the molecular in-plane orientation detected on the X-ray diffraction patterns.

Dielectric constants, which are estimated from the refractive indices, are summarized in Table V.[6] Depending on the backbone structures, ε_{xy} varies over 2.511 - 3.413 while ε_z changes over 2.484 - 2.684. ε_{av} is in the range of 2.502 - 3.132. $\Delta\varepsilon$ is 0.822 for PMDA-PDA PI, 0.808 for BPDA-PDA PI, 0.489 for ODPA-PDA PI, 0.446 for BTDA-PDA PI, and 0.027 for 6F-PDA PI.

In comparison, both n_{xy} and ε_{xy} follow the decreasing order BPDA-PDA PI > PMDA-PDA PI > ODPA-PDA PI > BTDA-PDA PI > 6F-PDA PI, respectively, whereas the n_z and ε_z are in the decreasing order BTDA-PDA PI > ODPA-PDA PI > BPDA-PDA PI > PMDA-PDA PI > 6F-PDA PI, respectively. In addition, the n_{av} and ε_{av} are in the decreasing order BPDA-PDA PI > PMDA-PDA PI > ODPA-PDA PI > BTDA-PDA PI > 6F-PDA PI, respectively.

Just counting dielectric properties, 6F-PDA PI is suitable for the applications in the microelectronic devices, owing to its relatively low refractive index and dielectric constant with almost negligible anisotropy.

Mechanical Properties

PMDA-PDA PI Derivatives. Mechanical properties of PI films, which were measured at room temperature by stress-strain analysis, are summarized in Table VI.[6,29,35] Young's modulus, which is the parameter of mechanical hardness, is highest for PMDA-PDA PI exhibiting the largest coherence length with irregular chain ordering. Such high modulus is reduced by incorporating short side groups into the polymer backbone: The modulus decreases in the order PMDA-PDA PI > PMDA-MEPDA PI > PMDA-MEOPDA PI > PMDA-CF3PDA PI. These moduli are correlated directly to the molecular packing coefficients, which are presented in Figure 6. Overall, higher modulus is originated from higher packing of polymer chains.[28,29,35,56] However, the reduction of modulus due to such side groups is relatively small. This means that the high modulus nature, which is the most advantageous property of PMDA-PDA PI rod, can be retained without large sacrifice through the incorporation of such short side groups.

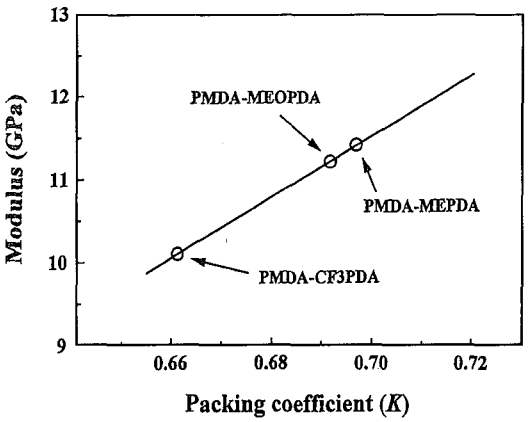

Figure 6. Correlationship between molecular packing coefficient and Young's modulus of PMDA-PDA PIs with side groups in thin films.

PMDA-PDA PI is very brittle. But the other PIs exhibit 197-292 MPa stress at break and 2.2-3.9% strain at break, depending on the side groups. In particular, the measured strains, which are an indicator of chain flexibility and toughness, are

Table VI. Mechanical Properties of PMDA-PDA PIs Containing Short Side Groups

PI Film[a]	Young's Modulus (GPa)	Stress at Break (MPa)	Strain at Break (%)
PMDA-PDA	12.2	-	
PMDA-MEPDA	11.4 (1.0)[b]	262 (26)	3.9 (0.8)
PMDA-MEOPDA	11.2 (0.3)	197 (12)	2.2 (0.6)
PMDA-CF3PDA	10.1 (1.5)	223 (10)	3.1 (0.4)

[a]Film thickness: 10-11.5 μm.

[b]The numbers in parentheses indicate 1 standard deviation.

Table VII. Mechanical Properties of PMDA-BZ PIs Containing Short Side Groups

PI Film[a]	Young's Modulus(GPa)	Stress at Break(MPa)	Strain at Break(%)
PMDA-BZ	11.1 (0.1)[b]	212 (13)	4 (1)
PMDA-MEOBZ	10.7 (0.1)	353 (28)	11 (1)
PMDA-MEBZ	9.9 (0.1)	345 (24)	12 (1)
PMDA-FBZ	9.2 (0.1)	200 (9)	4 (1)
PMDA-CF3BZ	7.6 (0.1)	293 (11)	21 (1)

[a]Film thickness: 9.3-14.3 μm.

[b]The numbers in parentheses indicate 1 standard deviation.

lower than the expected values. In general, both stress and strain at break are very sensitive to the quality of specimens including length-to-width ratio and defect levels in the specimen and its edges. In the measurement, PI films were prepared in a limited size, so that the length-to-width ratio of film strips was not large enough: only 25 mm length and 2.5 mm width. And, the film strips might have lots of crack-tips on their side edges. These might lead to the relatively low strains at break. Conclusively, there is confirmed indication that the brittleness of PMDA-PDA PI rod is improved by incorporating short side groups even though the strain at break was measured relatively small.

PMDA-BZ PI Derivatives. Table VII is a summary of mechanical properties of PMDA-BZ PI analogs.[30,32] PMDA-BZ PI exhibits 11.1 GPa modulus and 4% strain at break. The modulus is slightly lower than that (ca. 12.2 GPa) of PMDA-PDA PI. However, PMDA-BZ PI is relatively less brittle than PMDA-PDA PI. Considering chemical backbone structures, PMDA-BZ PI has one more phenylene moiety per the repeat unit than PMDA-PDA PI. The additionally inserted phenylene moiety may play a key role to promote the rotational freedom of the polymer chain, consequently improving the overall chain mobility that is critical to heal the mechanical brittleness.

A similar stress-strain curve is observed for the PMDA-FBZ PI. By the incorporation of fluoro side group into the polymer backbone, the low strain at break is not improved at all. In contrast, the other PIs with relatively bulky side groups show stress-strain curves that resemble that of a kink type of rigid BPDA-PDA PI that shows excellent mechanical properties. That is, the relative brittleness of PMDA-BZ PI is healed significantly by incorporating side groups bulkier than the fluoro group. The strain at break is 11-21%, depending upon the incorporated side groups. The effect of side group on the improvement of strain at break increases in the order H (hydrogen) $\approx$ F < $CH_3 \approx OCH_3$ < CF_3.

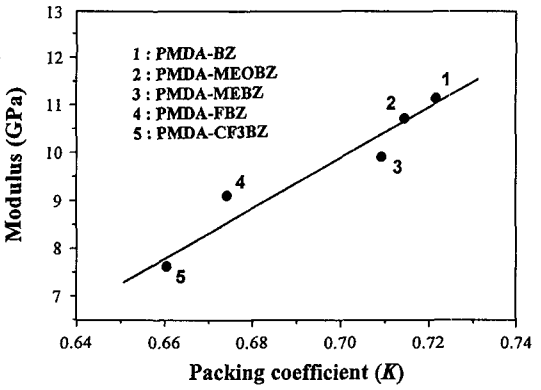

Figure 7. Correlationship between molecular packing coefficient and Young's modulus of PMDA-BZ PIs with side groups in thin films.

However, the modulus is reduced by incorporating side groups. The reduction of modulus is relatively large for the PMDA-CF3BZ PI, intermediate for the PMDA-MEBZ PI and PMDA-FBZ PI, and small for the PMDA-MEOBZ PI. These moduli are also dependent directly upon the molecular packing coefficients. As shown in Figure 7, higher molecular packing coefficient gives higher modulus: The modulus increases linearly with the molecular packing coefficient.

PDA-Based PI Derivatives. 6F-PDA PI is relatively weak and soft (see Table VIII).[6] The other three polyimides show excellent mechanical modulus, tensile strength and strain at break (see Table VIII).[6] However, BPDA-PDA and BTDA-PDA, which exhibited high chain ordering, reveal lower

Table VIII. Mechanical Properties of PDA-based PIs with Various Chain Rigidities

PI Film[a]	Young's Modulus(GPa)	Stress at Break(MPa)	Strain at Break(%)
BPDA-PDA	10.2 (0.2)[b]	597 (80)	47 (10)
ODPA-PDA	8.1 (0.2)	263 (20)	18 (11)
BTDA-PDA	7.1 (0.2)	248 (13)	18 (6)
6F-PDA	3.8 (0.07)	108 (20)	6 (3)

[a]Film thickness: 10.0-11.5 μm.

[b]The numbers in parentheses indicate 1 standard deviation.

modulus than that of PMDA-PDA. ODPA-PDA exhibits slightly higher modulus than that of BTDA-PDA in spite of its slightly lower coherence length with irregular ch ain ordering. In comparison, the modulus, which is the parameter of mechanical hardness, decreases in the order PMDA-PDA PI > BPDA-PDA PI > ODPA-PDA PI > BTDA-PDA PI > 6F-PDA PI. Strain at break follows the decreasing order BPDA-PDA PI > BTDA-PDA PI ≈ ODPA-PDA PI > 6F-PDA PI > PMDA-PDA PI. From these results, it is suggested that modulus, which is a mechanical charactersitic in the film plane, might result from both chain rigidity and in-plane orientation rather than chain ordering. Higher chain rigidity, which causes higher molecular in-plane orientation, produces higher in-plane modulus. In contrast to the modulus behavior, elongation at break is relatively large for biphenyl-linked BPDA-PDA PI and carbonyl-linked BTDA-PDA PI that exhibit high chain ordering. In addition, ether-linked ODPA-PDA PI in irregular chain ordering reveals strain at break comparable to that of BTDA-PDA PI. These results indicate that both the high chain ordering and the limited chain flexibility are reflected directly to the strain at break. Overall, BPDA-PDA PI exhibits exceptionally superior mechanical properties, except for its modulus lower than that of PMDA-PDA PI.

Thermal Properties

PMDA-PDA PI Derivatives. PMDA-PDA does not exhibit a glass transition temperature T_g below 500 °C.[6] However, T_g's of the other PIs are easily measurable using a dynamic mechanical thermal analyzer (DMTA).[29,35] T_g was determined to be 368 °C for PMDA-MEPDA PI, 365 °C for PMDA-MEOPDA PI, and 412 °C for PMDA-CF3PDA PI (see Table I). The results indicate that PMDA-PDA

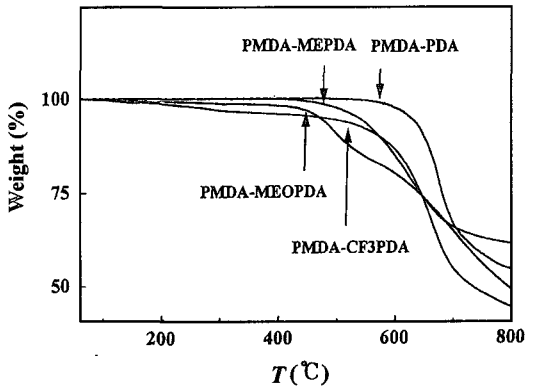

Figure 8. Thermogravimetric diagrams of PMDA-PDA PIs with side groups in thin films. The heating rate was 5.0 K/min. The measurement was conducted under nitrogen gas flow.

PI rod becomes flexible via incorporating short side groups into the backbone. Such improved chain flexibility is clued from the β-transition detected in the DMTA measurement. That is the β-transition due to the rotation along the C-N bond in the backbone is clearly detected to appear below 300 °C for all the PMDA-PDA PIs containing side groups.[29,35]

Thermal degradation starts over the range of 430-570 °C, depending upon the side groups (see Figure 8).[6,29,35] The results are listed in Table I. Degradation temperature T_d is in the decreasing order PMDA-PDA PI > PMDA-CF3PDA PI > PMDA-MEPDA PI > PMDA-MEOPDA PI .

As observed for PMDA-PDA PI, both PMDA-MEPDA PI and PMDA-CF3PDA PI exhibit one-step weight loss behaviors. This indicates that the side groups are thermally degraded together with the main chain. However, PMDA-MEOPDA PI reveals a two-step weight loss behavior. The weigh loss in the first step is almost equivalent to

the weight percentage of the methoxy side group to the total weight of the polymer. This weight loss is attributed to the thermal degradation of the methoxy side group. Then, the main chain part of the polymer is degraded in the second step at the high temperature region.

In-plane thermal expansion coefficients (TECs) were measured and averaged over the range of 100-200 °C. The results are presented in Table I.[6,29,35] PMDA-PDA PI exhibits 2.0 ppm/°C TEC, which is smaller than that (3.0 ppm/°C) of silicon wafer. In comparison, TEC increases in the order PMDA-PDA PI < PMDA-MEPDA PI < PMDA-MEOPDA PI < PMDA-CF3PDA PI. As aforementioned, the bulkiness of side group disturbs the molecular packing, consequently leading to an increase in the TEC: larger bulkiness of side group causes higher TEC in the polymer film.

In particular, PMDA-MEPDA shows a negative TEC. That is, this PI film is shrunken rather than expanded as the temperature increases. This behavior might relate to the characteristic of the film formation process. The PI film is spin-coated on substrates, followed by drying and imidization process. Through the film formation process the shrinkage takes place in the direction of film thickness and, however, is constrained in the film plane, because of the interfacial adhesion between the film and the substrate. This unidirectional shrinkage leads to relatively dense molecular packing in the direction of film thickness but loose molecular packing in the film plane. Both the dense molecular packing in the direction of film thickness and the loose molecular packing in the film plane are evident in the X-ray diffraction study described previously. PMDA-MEPDA PI is expected to have intrinsically very low TEC, so that the polymer chains loosely packed in the film plane undergoes shrinkage rather than expansion in the in-plane TEC measurement, resulting in a negative TEC. If this polyimide film is prepared in free-standing rather than on the substrate, it may exhibit a positively small TEC. Similar behavior is expected for the other polyimides but does not appear. This indicates that their TECs are relatively high enough to overcome such shrinkage, consequently resulting in positive TECs in the measurement.

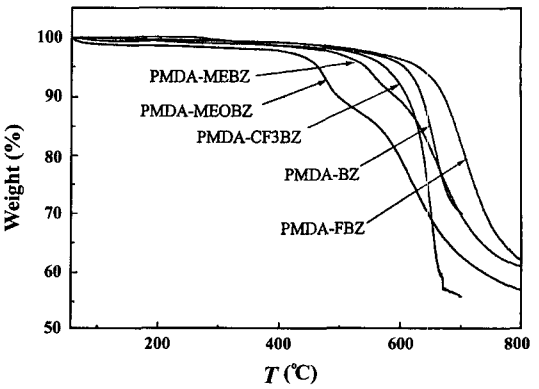

Figure 9. Thermogravimetric diagrams of PMDA-BZ PIs with side groups in thin films. The heating rate was 5.0 K/min. The measurement was conducted under nitrogen gas flow.

PMDA-BZ PI Derivatives. T_g's of PMDA-BZ PI analogs are summarized in Table II.[30,32] PMDA-BZ PI does not show T_g over the temperature window measured because of its high chain stiffness. The other PIs reveal glass transitions. In comparison, T_g is in the increasing order PMDA-MEOBZ PI < PMDA-MEBZ PI < PMDA-CF3BZ PI < PMDA-FBZ PI < PMDA-BZ PI.

These PIs also start to degrade over the range of 430-600 °C, depending upon the side groups (see Figure 9). For PMDA-BZ PI, PMDA-FBZ PI and PMDA-CF3BZ PI, one-step weight loss behaviors are observed. The results indicate that for these PIs the side groups are thermally degraded together with the main chain parts. However, both PMDA-MEOBZ PI and PMDA-MEBZ PI reveal a two-step weight loss behavior. In the first step the weight loss is almost equivalent to the weight percentage of the corresponding side group to the total weight of the polymer. The main chain part degrades in the second step at the high temperature region. Conclusively, methoxy and methyl side groups are more labile than the other side groups. In comparison, methoxy group is relatively more labile than methyl group. Thermal stability increases in the order PMDA-MEOBZ PI < PMDA-MEBZ PI < PMDA-CF3BZ PI < PMDA-BZ PI < PMDA-FBZ PI.

For PIs, TECs are measured and listed together in Table II.[30,32] All the PI films exhibit negative TECs. However, their absolute values are rela-

tively small. These mean that the PI films undergo shrinkage rather than expansion in the thermal treatment. The extent of shrinkage could be relatively small, but just slightly enough to overcome the expansion. These TEC behaviors are quite different from those of semiflexible and flexible PIs in films that show positively high TECs. Such negative TECs may be associated with residual stresses built during the film formation process. That is, these PIs are linear and highly rigid, so that they have relatively high T_g in spite of the incorporated side groups. For this, residual stress, which is built during film formation, could not be removed completely by the preheating process, consequently causing small negative TEC in the film.

In comparison, the absolute value of the negative TEC is in the increasing order PMDA-BZ PI ≈ PMDA-FBZ PI < PMDA-MEOBZ PI≈PMDA-CF3BZ PI < PMDA-MEBZ PI. This indicates that incorporating bulkier side group into the backbone causes relatively higher shrinkage in the film. However, PMDA-MEBZ PI shrinks more than PMDA-MEOBZ PI and PMDA-CF3BZ PI in spite of its methyl side group smaller than methoxy and trifluoromethyl groups.

PDA-Based PI Derivatives. T_g appears at 320 °C for BPDA-PDA PI, 270 °C for ODPA-PDA PI, 370 °C for BTDA-PDA PI, and 360 °C for 6F-PDA PI.[6] 6F-PDA PI shows a relatively sharp glass transition, whereas the other three polyimides exhibited very broad transition. In particular, the glass transition of ODPA-PDA PI, which shows irregular ordering of chains, is very broad compared with those of BPDA-PDA PI and BTDA-PDA PI which exhibit high chain ordering. In addition, all polyimides except for PMDA-PDA PI show a typically broad relaxation peak over 100-300 °C, which corresponds to the mixed β- and β'-relaxations due to phenyl moieties on the backbone and moisture absorbed in films, respectively, as observed in most aromatic polyimides. This broad relaxation peak apparently does not appear for PMDA-PDA. It might result from highly restricted motions of the phenyl moieties and moisture in the highly supercooled state of the fully rodlike PMDA-PDA PI that is under a limited cyclic deformation due to its high modulus during the DMTA measurement.

These PIs are thermally stable up to > 500 °C. In addition, TECs were characterized as follows.[6] TEC is 7.5 ppm/ °C for BPDA-PDA PI, 30 ppm/°C for BTDA-PDA PI, 35 ppm/°C for ODPA-PDA PI, and 48 ppm/°C for 6F-PDA PI. That is, TEC is in increasing order PMDA-PDA PI < BPDA-PDA PI < BTDA-PDA PI < ODPA-PDA PI < 6F-PDA PI.

BPDA-PDA PI and BTDA-PDA PI, which exhibit excellent ordering of chains, reveal relatively larger TECs than PMDA-PDA PI with a poor lateral packing order. This suggests that the chain rigidity is the more critical factor to control TEC than the chain order. However, ODPA-PDA PI, which shows slightly higher chain rigidity and irregular chain order, exhibits slightly larger TEC than BTDA-PDA PI. This indicates that for polyimides having moderate chain rigidities, such as ODPA-PDA PI and BTDA-PDA PI, the chain order is also the important factor to control TEC: that is, higher chain order leads lower TEC. In conclusion, TEC is influenced primarily by chain rigidity and secondarily by chain order. Overall, higher coherence length along the chain axis, which depends on the chain rigidity and the chain order, causes lower TEC. That is, lower TEC, which is in-plane characteristic, can be achievable for polymer that exhibits higher rigidity and ordering of chain accompanied with high degree of molecular in-plane orientation in films.

Conclusions

First, by incorporating short side groups, the mechanical brittleness in PMDA-PDA PI and PMDA-BZ PI was healed with an only small portion of sacrifice in the modulus. The side groups enhance the ordering of PI rods, leading to a bundle like molecular ordering. The improvement in the brittleness is attributed mainly to the chain mobility and lateral chain packing order enhanced by the side groups. On the other hand, the side groups are relatively small but still have a limited bulkiness, so that they cause a reduction in the packing efficiency of polymer chains. These side groups affect further properties in either postive way or negative way. That is, refractive indices, dielectric constants, and their anisotropies reduce.

Both glass transition and thermal degradation temperatures lower too. And, thermal expansivity becomes large.

Second, by incorporating kink or flexible linkages, the mechanical brittleness was also healed. However, the sacrifice of modulus is dependent strongly on the sort of linkage. Both kinked BPDA -PDA PI and bent BTDA-PDA PI exhibit high molecular ordering while bent ODPA-PDA PI shows poor molecular ordering. 6F-PDA PI, which has isopropyl links and bulky trifluoromethyl groups, was structureless. Higher chain rigidity and order produce higher in-plane orientation of chains in films. Higher molecular in-plane orientation causes significantly higher anisotropies in refractive indices and dielectric constants, higher modulus, and lower TEC.

In conclusion, the mechanical brittleness of aromatic polyimide rods was successfully improved with keeping the high modulus by incorporating both short side groups and kink (or bent) linkages. In order to minimize the sacrifice of the advantageous properties, the side group is limited to methyl, methoxy, and trifluoromethyl, while the linkage is limited to kinked biphenyl, ether, and carbonyl.

Acknowledgments. The authors acknowledge the supports of the Center for Integrated Molecular Systems (KOSEF) and of the Ministry of Education (Brain Korea 21 Program).

References

(1) W. M. Edwards and I. M. Robinson, *U.S. Patent* 2,867,609 (1959).
(2) J. A. Kreuz, *US Patent* 3,271,366 (1966).
(3) C. E. Sroog, *Prog. Polym. Sci.*, **16**, 561 (1991).
(4) M. I. Bessonov and V. A. Zubkov (eds.), *Polyamic acids and Polyimides: Synthesis, Transformations, and Structure,* CRS, Boca Raton, LA, 1993.
(5) K. L. Ghosh and K. L. Mittal (eds.), *Polyimides: Fundamentals and Applications,* Dekker, New York, 1996.
(6) M. Ree, K. Kim, S. H. Woo, and H. Chang, *J. Appl. Phys.*, **81**, 698 (1997).
(7) M. Ree, S. H. Woo, K. Kim, H. Chang, W. C. Zin, K. B. Lee, and Y. J. Park, *Macromol. Symp.*, **118**, 213 (1997).
(8) S. Numata, K. Fujisaki, and N. Kinjo, *Polymer,* **28**, 2282 (1987).
(9) A. S. Argon and M. I. Bessonov, *Polym. Eng. Sci.*, **17**, 174 (1977).
(10) H. Ishida, S. T. Wellinghoff, E. Baer, and J. L. Koenig, *Macromolecules,* **13**, 826 (1980).
(11) S. T. Wellinghoff, H. Ishida, J. L. Koenig, and E. Baer, *Macromolecules,* **13**, 834 (1980).
(12) J. R. Havens, H. Ishida, and J. L. Koenig, *Macromolecules,* **14**, 1327 (1981).
(13) M. Ree, D. Y. Yoon, and W. Volksen, *J. Polym. Sci.: Part B: Polym. Phys.*, **29**, 1203 (1991).
(14) M. Ree, D. Y. Yoon, and W. Volksen, *Polymer Preprints,* **31**(1), 613 (1990).
(15) S. Rojstaczer, M. Ree, D. Y. Yoon, and W. Volksen, *J. Polym. Sci.: Part B: Polym. Phys.*, **30**, 133 (1992).
(16) Y. Kim, M. Ree, T. Chang, C. S. Ha, T. L. Nunes, and J. S. Lin, *J. Polym. Sci.: Part B: Polym. Phys.*, **33**, 2075 (1995).
(17) M. Ree, T. L. Nunes, and K.-J. R. Chen, *J. Polym. Sci.: Part B: Polym. Phys.*, **33**, 453 (1995).
(18) J. K. Gillham and H. C. Gillham, *Polym. Eng. Sci.*, **13**, 447 (1973).
(19) M. Kochi, S. Isoda, R. Yokota, and H. Kambe, *J. Polym. Sci.: Part B: Polym. Phys.*, **24**, 1619 (1986).
(20) E. Butta, S. De Petris, and M. Pasquini, *J. Appl. Polym. Sci.*, **13**, 1073 (1969).
(21) W. Wrasidlo, *J. Macromol. Sci.-Phys.*, **B3**, 559 (1972).
(22) R. R. Tummala and E. J. Rymaszewski (eds.), *Microelectronics Packaging Handbook,* van Nostrand Reinhold, New York, 1989.
(23) L. F. Thompson, C. G. Willson, and S. Tagawa (eds.), *Polymers for Microelectronics: Resists and Dielectrics (ACS. Symp. Ser. Vol. 537),* Am. Chem. Soc., Washington, DC., 1994.
(24) A. Deutsch, M. Swaminathan, M. Ree, C. Surovic, G. Arjavalingam, K. Prasad, D. C. McHoerron, M. McAllister, G. V. Kopcsay, A. P. Giri, E. Perfecto, and G. E. White, *IEEE Trans. Comp. Packag. Manuf. Technol.: Part B: Adv. Packaging,* **17**(4), 486 (1994).
(25) G. Czornyj, K. J. Chen, G. Prada-Silva, A. Arnold, H. A. Souleotis, S. Kim, M. Ree, W. Volksen, D. Dawson, and R. DiPietro, *Proc. Elect. Comp. Tech. (IEEE),* **42**, 682 (1992).
(26) G. L. Slonimskii, A. A. Askadskii, and A. I. Kitaigorodski, *Vyskomol. Soyed.*, **A12**, 494 (1970).
(27) S. Numata, S. Oohara, K. Fujisaki, J. Imaijumi, and N. Kinjo, *J. Appl.Polym. Sci.*, **31**, 101 (1986).
(28) K. Yamada, T. Mitsutake, K. Hiroshima, and T. Kajiyama, *Proc. 2nd SPSJ Int. Polym. Conf. Tokyo,* Aug. 20, 1986, pp 51.
(29) S. I. Kim, T. J. Shin, S. M. Pyo, J. M. Moon, and M. Ree, *Polymer,* **40**, 1603 (1999).
(30) S. M. Pyo, S. I. Kim, T. J. Shin, Y. H. Park, and M. Ree, *J. Polym. Sci.: Part A: Polym. Chem.*, **37**, 937

(1999).
(31) K. Kim, Ph.D. Thesis, Pohang University of Science & Technology, 1997.
(32) S. M. Pyo, M.S. Thesis, Pohang University of Science & Technology, 1998.
(33) K. H. Lee, Ph.D. Thesis , Pohang University of Science & Technology, 1998.
(34) H. Kim, Ph.D. Thesis , Pohang University of Science & Technology, 1997.
(35) S. I. Kim, Ph.D. Thesis , Pohang University of Science & Technology, 1999.
(36) S.-B. Park, H. Kim, W.-C. Zin, and J. C. Jung, *Macromolecules,* **26**, 1627 (1993).
(37) J. C. Jung, and S.-B. Park, *Polymer Bulletin,* **35**, 423 (1995).
(38) J. C. Jung and S.-B. Park, *J. Polymer Sci.: Part A: Polymer Chem.,* **34**, 357 (1996).
(39) H. Kim, J. C. Jung, and W.-C. Zin, *Polymer,* **37**, 2573 (1996).
(40) H. G. Rogers, R. A. Gaudiana, W. C. Hollinsed, P. S. Kalyanaraman, J. S. Manello, C. McGowan, R. A. Minns, and R. Sahatjian, *Macromolecules,* **18**, 1058 (1985).
(41) K. H. Lee and J. C. Jung, *Polymer Bulletin,* **40**, 407 (1998).
(42) S. W. Lee, S. I. Kim, Y. H. Park, M. Ree, K. H. Lee, and J. C. Jung, *Liquid Cryst. Mol. Cryst.,* **349**, 271 (2000).
(43) T. Matsuura, M. Ishizawa, Y. Hasuda, and S. Nishi, *Macromolecules,* **25**, 3540 (1992).
(44) K. Kim and M. Ree, *J. Polym. Sci.: Part A: Polym. Chem.,* **36**, 1755 (1998).
(45) S. Scherrer, *Nachr. Gottinger Gesell,* **2**, 98 (1918).
(46) G. L. Slonimskii, A. A. Askadskii, and A. I. Kitaigorodski, *Vyskomol. Soyed.,* **A12**, 494 (1970).
(47) D. Y. Yoon, W. Volksen, L. Depero, W. Parrish, and M. Ree, *Mat. Res. Soc. Symp. Proc.,* **227**, 371 (1991).
(48) M. Ree, S. Depero, D. Y. Yoon, and W. Parrish, to be published.
(49) W. Kuhn, *Kolloid-Z.,* **76**, 258 (1936).
(50) T. M. Birshtein and A. N. Goryunov, *Vysokomol. Soyed.,* **A21**, 1990 (1979); *Polym. Sci. USSR,* **21**, 2196 (1980).
(51) W. H. Goh, K. Kim, and M. Ree, *Korea Polymer J.,* **6**, 241 (1998).
(52) H. Han and M. Ree, *Korea Polymer J.,* **5**, 152 (1997).
(53) W. Groh and A. Zimmerman, *Macromolecules,* **24**, 6660 (1991).
(54) J. C. Maxwell, *N. Philos. Trans.,* **155**, 459 (1865).
(55) C.C. Ku and R. Liepins (eds.), *Electrical Properties of Polymers: Chemical Principles,* Hanser, New York, 1987.
(56) S. Numata, K. Fujisaki, and N. Kinjo, *Polymer,* **28**, 2282 (1987).